SECTION I
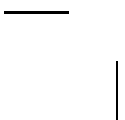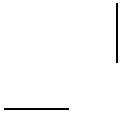
SUPRAMOLECULAR OBJECTS TOWARDS MULTI-TASK ORGANIC MATERIALS

SUPRAMOLECULAR MATERIALIZATION OF FULLERENE ASSEMBLIES

Sukumaran S. Babu,[1] *Hidehiko Asanuma,*[2] *and Takashi Nakanishi*[1]

[1]National Institute for Materials Science, Sengen, Tsukuba, Japan
[2]Max Planck Institute of Colloids and Interfaces, Potsdam, Germany

1.1 INTRODUCTION

Self-organization of molecules using various supramolecular interactions has gained much attention in past decades because a large number of versatile assemblies have been created with excellent and tunable properties [1–3]. Hence, it is particularly important to study the various aspects of supramolecular chemistry, including soft functional assemblies [4]. The crucial and deciding factors while assembling molecules in a regular pattern are satisfied by the incorporation of suitable functional moieties [4]. It enables the molecules to recognize and self-organize in a programmed manner to gather amended properties, which is not attainable as monomers [5]. The reversibility of functional properties through monomer–aggregate transition is always an inspiration for scientists to design new functional assemblies. The challenging task is the control over the self-organization, whereby morphologies with defined size and shape are to be tuned. The incorporation of various hydrogen bonding units, ionic groups, chiral directing moieties, and solubility-controlling alkyl/glycol chains to various π-conjugated, commonly planar, chromophores such as oligo(p-phenylenevinylene)s (OPVs), perylene- or merocyanine-type dyes, porphyrins, hexabenzocoronene (HBC), and dendritic type mesogens enabled precise control over assembly formation [4].

Meijer *et al.* have shown that the incorporation of various self-recognition as well as hydrogen bonding units and various alkyl side chains resulted in functional OPV assemblies [6]. Interestingly, these assemblies acted as a good medium for energy or electron transfer studies [7]. In addition, this resulted in

the formation of assemblies with exciting supramorphologies [8]. Reports from the group of Ajayaghosh showed that the OPV scaffold is adequate for facile energy transfer mediated by tunable organogel medium with enhanced emission [9]. Organogelation of a series of OPVs with different end functional groups, which are donors (D) and acceptors (A), enabled tuning of the excited state properties, resulting in white-light-emitting organogels [10]. Würthner *et al.* have contributed much in the area of self-organization of perylene- and merocyanine-based dyes [11]. The extensive studies have shown that different self-assembled dyes with near-infrared (NIR) absorption features are potential candidates in creating supramolecular assemblies and applications in organic photovoltaic devices [12]. Aida and coworkers have studied the self-assemblies and functional properties of HBC [13]- and porphyrin [14]-based systems. Self-organization of amphiphilic HBC molecules has led to HBC nanotubes, which may find direct application in organic devices. Recently, the incorporation of various functional chromophores in the liquid crystalline assemblies have also been extensively studied [15].

Apart from the flat planar π-systems, self-organization of spherical π-systems such as fullerenes (C_{60} and C_{70}) have also been vastly studied in the past decades [16]. The abundant and unique optoelectronic properties of the curved π-surface of C_{60} has been utilized for the sensible design of inexpensive, lightweight, and durable organic photovoltaic devices [17]. The functionalization of fullerenes, reactive owing to its enhanced curvature, using different synthetic protocols resulted in a large number of derivatives with exceptionally good electron transfer and self-assembly properties [18]. The research area of fullerene self-assembly has formulated new dimensions through molecular design. Here, we focus on the new concept of hydrophobic amphiphilicity, which gained much attention recently [19].

1.2   HYDROPHOBIC–AMPHIPHILIC CONCEPT

The concept of molecular amphiphilicity is one of the widely exploited strategies in the area of interface science because of the versatile features of self-assembly [20]. Amphiphilic molecules consist of hydrophobic (hydrocarbon moiety) and hydrophilic units (charged anionic/cationic groups or uncharged polar groups), which can exhibit a large number of supramolecular architectures, such as micelles, vesicles, lamellae, tubular arrangements, as well as various cubic phases, depending on the relative balance between hydrophobic and hydrophilic interactions and on the solvophobic conditions [21–23]. The concept of amphiphilicity has been studied deeply in surfactants, detergents, and oils, and has great implications toward chemistry, biochemistry, biophysics, and colloid science [24]. The structural features of an amphiphile enable it to aggregate in an aqueous environment through aggregation of the hydrophobic apolar tails, which are protected from water by polar heads.
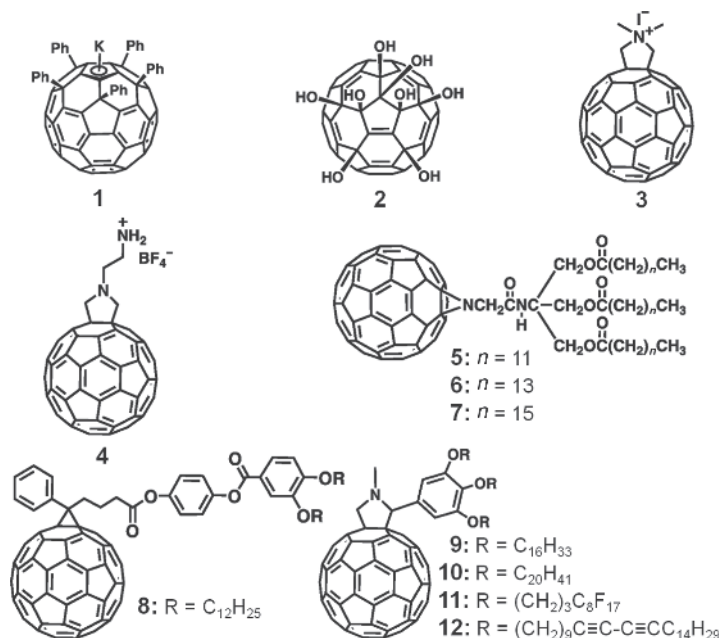
Scheme 1-1   Chemical structures of potassium salts of pentaphenyl fullerene (**1**), C_{60}-N,N-dimethylpyrrolidinium iodide (**2**), octahydroxy fullerene (**3**), fullerene containing ammonium cation and BF^{4-} counter anion (**4**), C_{60} derivatives consisting of three alkyl chains with an amide and three ester groups (**5–7**), C_{60}-didodecyloxybenzene dyad (**8**), fulleropyrrolidine functionalized with 3,4,5-alkyloxyphenyl groups (**9, 10**), 3,4,5-semiperfluoroalkyl (**11**), and diacetylene (**12**) groups.

The research interest regarding self-assembly behaviors of amphiphilic fullerenes has been significantly increased. Reports from the group of Nakamura have shown that a potassium salt of pentaphenyl C_{60} (**1**) (Scheme 1-1) forms vesicles in aqueous conditions [25]. Zhang *et al.* reported that another amphiphile, octahydroxy C_{60} (**2**) (Scheme 1-1), forms spherical aggregates in water with a hydrodynamic radius R_h of about 100 nm [26]. Tour and coworkers investigated the self-assembly of C_{60}-N,N-dimethylpyrrolidinium iodide (**3**) (Scheme 1-1) leading to the formation of 1-D nanorods and vesicles under various experimental conditions [27]. Later, Shiga *et al.* studied the self-assembly of **3** in binary liquid mixtures of toluene and iodomethane, which resulted in the formation of nanosheets and precipitation as nanofibers in toluene/dimethyl sulfoxide (DMSO) mixture [28]. Interestingly, the matted nanosheets, several micrometers in length and about 100 nm in thickness, were formed from a large number of nanorods of 20-nm diameter. Another report from the group of Prato showed that C_{60} derivative with a short aliphatic chain containing an ammonium cation and a counter anion, BF_4^- (**4**), forms well-ordered nanorod-like aggregates in water [29]. All the above examples are less extended in shape and morphology.

In this context, a concept of "hydrophobic amphiphilicity" will be considered [19]. The structural modification of an amphiphile that relies on hydrophobic–hydrophobic balance has added a new dimension to amphiphilicity. The relative balance between two hydrophobic interactions, namely, $\pi-\pi$ (C_{60}) and van der Waals (alkyl chains), enabled delivery of diverse nano and microscopic architectures (supramolecular polymorphism) [30], which are never observed in the case of conventional amphiphilic fullerenes. A clear evidence of solvophobicity is exhibited by this C_{60}-based hydrophobic amphiphiles, leading to supramolecular assemblies with tunable properties and morphology.
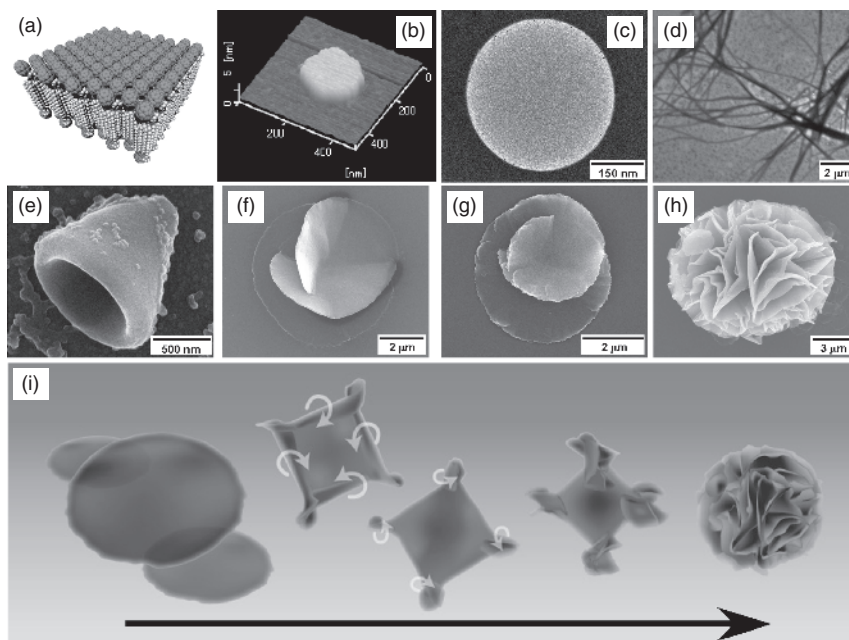
1.3 SUPRAMOLECULAR ASSEMBLIES OF C_{60}-BEARING ALIPHATIC CHAINS

Nakashima and coworkers have reported C_{60} derivatives that bear three alkyl chains with an amide and three ester connectors (**5**–**7**, Scheme 1-1) [31–33]. These molecules lack the high hydrophilic nature of the conventional C_{60} amphiphiles and hence are soluble in various organic solvents. More interestingly, although the molecules are mainly composed of hydrophobic C_{60} and aliphatic chains, they were capable of forming Langmuir films on water, which behaves similar to lipid biomembranes [33]. Patnaik and coworkers reported the self-assembly of a partially ground-state charge-separated nonpolar–polar–nonpolar fullerene(C_{60})-didodecyloxybenzene dyad (**8**) (Scheme 1-1) to form micrometer-sized rod/sheet-like aggregates and in-plane bilayer vesicles with a head-to-head C_{60} packing conformation [34,35].

In addition, a series of alkylated C_{60} derivatives synthesized in our laboratory have exhibited interesting assembly phenomena when compared to the other alkylated C_{60} derivatives [36]. The relative balance of two hydrophobic interactions derived from C_{60} (less hydrophobic) and alkyl chains (more hydrophobic) [19] has resulted in dimensionally controlled supramolecular architectures with interesting assembly properties. Detailed assembly studies have revealed that this multi(alkyloxy)-phenyl substituted fulleropyrrolidines show supramolecular polymorphism in different organic solvents.

1.3.1 Hierarchical Supramorphology

The self-assembly of fulleropyrrolidine functionalized with a 3,4,5-tri(hexadecyloxy)phenyl group (**9**) exhibited supramolecular polymorphism: formation of different well-defined self-organized superstructures in various solvents and experimental conditions (Fig. 1-1) [30]. It is remarkable that a delicate balance between the hydrophobic interaction of chemically different C_{60} and saturated hydrocarbon chains drives the molecules to nanostructures with various interesting morphologies. The C_{60} composed of carbon atoms with sp^2 hybrid orbitals exhibits high affinity toward aromatic solvents (benzene, toluene, and xylenes), whereas the saturated hydrocarbon part consists of sp^3 hybridized carbons that have a higher affinity to alkanes than the aromatic compounds.

Figure 1-1 (a) The proposed structural model of bilayer assembly with interdigitated alkyl chains. (b) AFM image of disc-shaped assemblies of **9** formed in 1,4-dioxane as a precursor of the flower-shaped supramolecular assembly (h). SEM images of supramolecular assemblies of **9**, (c) spherical, (d) fibrous, (e) conical, (f) left-handed, and (g) right-handed spiral objects obtained from various solvent conditions. (i) Schematic representation of the formation mechanism of the flower-shaped supramolecular assembly. *Source:* Reprinted with permission [30,37].

This preferential affinity of the aromatic and aliphatic moieties toward different solvents is the basis of the unusual amphiphilicity observed in the molecular assemblies of C_{60} derivatives that bear aliphatic chains.

Self-assembled supramolecular objects were prepared by evaporation to dryness of a 1 mL chloroform solution of **9** ([**9**] = 1.0 mM) followed by the addition of 1 mL of solvents with different polarities. The field emission scanning electron microscopic (FE-SEM) images of the light brown mixtures from the respective solvents after heating at 60–70°C for 2 h indicated that **9** self-assembles into hierarchically ordered nano- and micro-superstructures [30]. It is assumed that the self-organization starts with a bilayer structure of self-assembled interdigitated bilayer of **9**, in which aromatic C_{60} layers in the upper and lower parts are separated by an aliphatic chain layer (Fig. 1-1a). Interestingly, when 1,4-dioxane is used for self-assembly, 2-D self-organized single bilayer discs (Fig. 1-1b) with diameters of 0.2–1.5 μm were obtained. In the case of 2-propanol/toluene system, **9** forms spherical aggregates with an average diameter of 250 nm (Fig. 1-1c). Fibers with partially twisted tapes appeared in 1-propanol (Fig. 1-1d), whereas conical objects with a diameter of 60 nm and perforated at

the cone apex were developed from H_2O-tetrahydrofuran (THF) mixture (1:1) (Fig. 1-1e). In addition, left-handed spiral microstructures were obtained from 2-(R)-butanol (Fig. 1-1f), whereas 2-(S)-butanol provided right-handed spiral objects (Fig. 1-1g) of 3 to 6 μm diameter. The hierarchical organization of **9** on cooling down the 1,4-dioxane solution from 60 to 20°C, followed by cooling to 5°C, resulted in microscopic flowerlike superstructures (Fig. 1-1h) 3–10 μm in size, with crumpled-sheet-like or flakelike nanostructures of several tens of nanometers in thickness [37]. Figure 1-1i explains the transformation (shape shift) mechanism from assembled molecular bilayer discs to microscopic flower-shaped superstructures of the alkyl-conjugated C_{60}-derivative **9**. In order to understand the mechanism and intermediate assembly structures of the flowerlike objects in detail, a homogeneous 1,4-dioxane solution of **9** was cooled rapidly from 60 to 5°C. Interestingly, preformed disc objects were loosely rolled up at the edges (Fig. 1-1i). The rolling distortions at every quarter of the disc resulted in square-shaped objects having four corners with conical shapes developed by the encounter of the rolled or folded edges on the discs. As rolling up proceeds continuously, spatial congestions at the four corners lead to crumpling, bending, stretching, and fracture of the discs. Immediately after these transformations, the bilayer growth at the edges continues which fixes the spatial conformation of the crumpled sheets, and finally leads to the formation of flower-shaped superstructures (Fig. 1-1i) [37].

In order to characterize the self-organized objects, various optical, morphological, and analytical experimental techniques have been utilized. At first, the assemblies were observed through an optical microscope to confirm the formation and further the nano-micrometer-sized structures. A more magnified analysis was carried out by scanning electron microscopy (SEM). To get a clear approximation of the organization at the molecular level, X-ray diffraction (XRD) and transmission electron microscopy (TEM and cryo-TEM) experiments were performed. In our case, the bimolecular layer assembles through alkyl chain interdigitation. Analytical experiments such as differential scanning calorimetry (DSC) to understand the thermal phase transitions and stability of the assembly and optical measurements using UV-vis spectroscopy to monitor the $C_{60}-C_{60}$ interaction and FT-IR to record the alkyl chain conformation have been commonly used. The surface topography of the resulted assembly structures were observed through atomic force microscope (AFM) and occasionally by scanning tunneling microscope (STM) imaging [38–40].

### 1.3.2   Antiwetting Architectures

Antiwetting feature is a fundamentally important phenomenon. The tendency of water molecules to exclude or move away from nonpolar molecules leads to marginal segregation between water and nonpolar substances. The crucial deciding factor is the surface roughness of the nonpolar surface on which water is spread. A surface with micro- and nanostructured roughness generates

superhydrophobicity with a water contact angle (CA) greater than $150°$; the air is trapped between the surface and water droplets [41]. The development of functional assemblies of C_{60} with antiwetting properties is of considerable significance in current research interest because of the applications in durable organic devices. In this context, the well-defined three-dimensional (3-D) fractal architectures of alkyl-conjugated C_{60} find useful applications using the morphological features. Self-organization of a C_{60} derivative 10 (Scheme 1-1) with 3,4,5-tri(eicosyloxy)phenyl group in 1,4-dioxane solution led to spontaneous formation of micrometer-sized globular objects with wrinkled nanoflake structures at the outer surface (Fig. 1-2a) [42]. The dewetting ability of the globular objects was investigated by measuring the static water contact angle of the superhydrophobic surface obtained from **10**. Interestingly, in the case of globular objects, a water contact angle of $152°$ (inset of Fig. 1-2a) was observed, whereas a simple spin-coated film prepared from a homogeneous chloroform solution of **10** exhibited a static water contact angle of about $103°$. The unique geometry of the "nano"-flakelike "micro" particles possesses tiny pockets at the surface that entrap air inside, exhibit two-tier roughness, and enhance the surface hydrophobicity. One of the advantages of these superhydrophobic systems is the reusability; the prepared thin films can readily be recovered by dissolving them in chloroform and reused.

It is a crucial question whether the C_{60} or the alkyl tails of **10** is exposed to the outer surface. In order to understand this, nano-flakelike microparticles of **10** have been prepared from the nonpolar solvent n-dodecane (Fig. 1-2b), which exhibited a static water contact angle of $164°$ (inset of Fig. 1-2b). This contact angle value is higher than that of the assembly prepared from the polar solvent 1,4-dioxane ($152°$, Fig. 1-2a), indicating that in the case of assemblies in a polar solvent, such as 1,4-dioxane, C_{60} moieties are exposed to the outer surface. The hydrocarbon tails are more hydrophobic than the moderately hydrophobic C_{60} moiety [19,33], and hence, owing to the mutual affinity, the outer surface components of the assembly of **10** from n-alkane solvents are presumably composed of the hydrocarbon tails [43]. This observation was further confirmed by the static water contact angle of the fractal-shaped microparticles ($\sim148°$) (Fig. 1-2c) of the fluoroalkyl conjugated C_{60} derivative (**11**, Scheme 1-1) assembled in a polar solvent, that is, diethoxyethane. The C_{60} moieties are exposed to the outer surface of the nanoflaked microparticles prepared from polar solvent conditions.

Even though the self-assembled objects exhibit an interesting surface morphology with water repellent properties, the robustness of the assemblies still remains a challenge. This may limit the potential use of these and most of the self-assembled organic objects for practical applications. In order to overcome this difficulty, C_{60} equipped with alkyl chains containing photo cross-linker (diacetylene) was synthesised (**12**, Scheme 1-1) [44]. UV light irradiation of the flakelike microparticles of **12** (Fig. 1-2d) resulted in the polymerization of both diacetylene and C_{60} moieties (Fig. 1-2e) and enabled getting chemically and mechanically robust assemblies (>29-fold compared to the nonpolymerized one) with antiwetting property (inset of Fig. 1-2d).
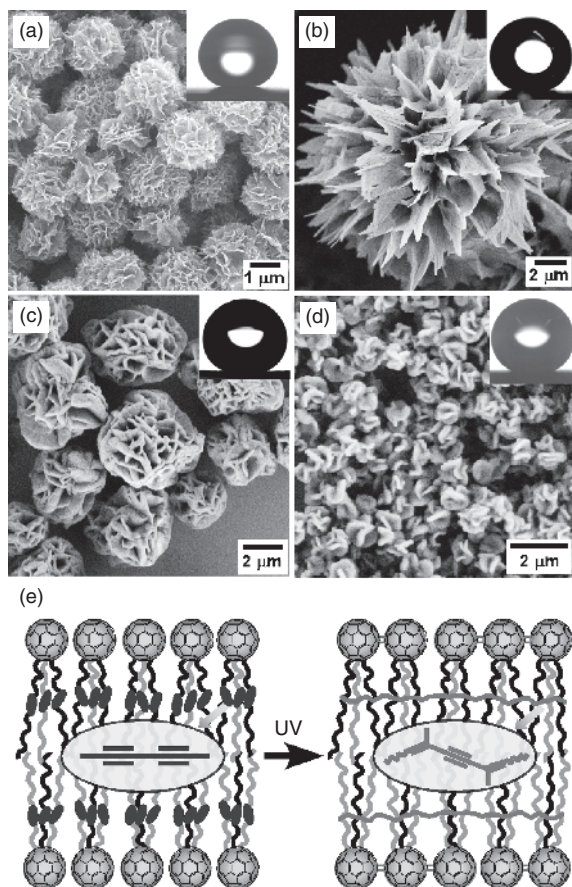
Figure 1-2 SEM images of flower-shaped supramolecular assemblies of **10** from (a) 1,4-dioxane and (b) *n*-dodecane, (c) **11** from diethoxyethane, (d) **12** from THF/MeOH mixture. Insets show the photographs of a water droplet on the surface with static water contact angles (a) 152°, (b) 164°, (c) 148°, and (d) 146°. (e) Schematic representation of the photo-cross-linking process in the bilayer structural subunit of **12**. *Source:* Reprinted with permission [42–44].

1.4 FUNCTIONS ORIGINATED FROM THREE-DIMENSIONAL FLAKELIKE MICROPARTICLES

One of the challenging tasks in the case of supramolecular architectures created by the self-assembly approach is to find out suitable applications. As a new strategy, reports from our group have shown how best the assemblies can be effectively utilized. Two unique approaches have been implemented to diversify the applications.

1.4.1 Supramolecular Molding Method

The remarkable and reliable method to develop well-designed hard matter using molecularly assembled supramolecular soft matter is by metallization. Interestingly, supramolecular architectures with structural and morphological diversity can deliver a broad range of high-definition templates for the design and synthesis

of unusual functional inorganic nanoarchitectures. In this direction, transcription of C_{60}-based microparticles having flakelike outer surface features obtained through self-assembly into various metals was demonstrated [45]. The sputtering of the desired metal (Au, Pt, Ti, and Ni) directly onto a thin film of the supramolecular assemblies, followed by the removal of the C_{60} template using organic solvents, enabled successfully transferring the self-assembled features directly on to the metal surfaces (Fig. 1-3a). The advantage of this transcription method is the possibility of recovering and reusing the template, making the entire process sustainable. In order to understand the features of the nanostructured metal surfaces, it has been applied in surface-enhanced Raman experiments. For example, surface-enhanced Raman scattering (SERS) of the resulting metal Au nanoflake exhibited an enhancement factor on an order of 10^5. This study has revealed a simple method for the transcription of the morphological features
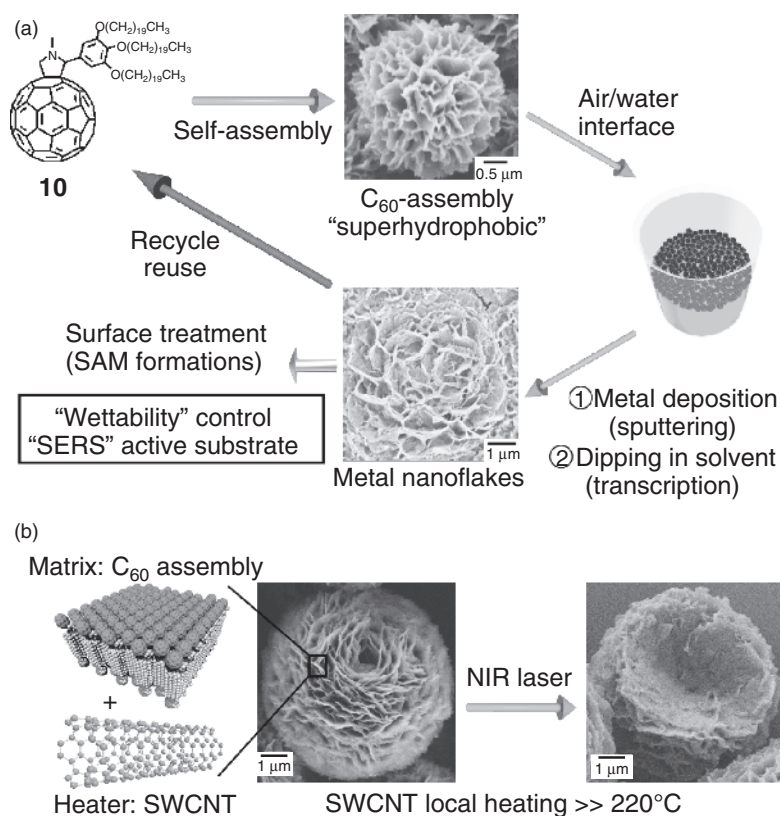
Figure 1-3 (a) Schematic representation for the preparation of metal nanoflake surfaces by using supramolecular architectures of **10** as templates. (b) Scheme of the coassembly of **10**-SWCNT for evaluating photothermal conversion of SWCNT; SEM images before (left) and after (right) illumination by an NIR laser (50 mW). *Source:* Reprinted with permission [45,48].

of a self-assembled object directly to different active metal surfaces, which has useful applications [46].

1.4.2   Thermal Indicator for NIR-Induced Local Heating of Carbon Nanotube

A promising strategy for assessing temperature rise during photothermal conversion of single-walled carbon nanotube (SWCNT) on NIR irradiation [47] was demonstrated by microparticles obtained by the coassembly of **10** and SWCNT (Fig. 1-3b) [48]. The flake-shaped microparticles of **10**-SWCNT were prepared by heating 1,4-dioxane solution of **10** and SWCNT to 70°C with ultrasonication followed by cooling to room temperature. On irradiation with NIR laser of lower intensity (50 mW), the microparticles started to deform (Fig. 1-3b), and when the laser intensity was increased to 90 mW, they were destroyed immediately. The flake-shaped surfaces of **10-**SWCNT assemblies have a mesomorphic-to-isotropic transition (melting point) at 191.8°C. Interestingly, microdisc (**9**-SWCNT, 2–8 μm) and flake-shaped microparticles (**13**-SWCNT, 2–4 μm) with melting points of 217.2 and 223.0°C, respectively, were also deformed on NIR laser illumination. This study demonstrates that NIR irradiation of C_{60}-SWCNT assembly can reach a local heating temperature in excess of around 220°C. The advantage of this system is the possibility of *in situ* visualization of deformation during photothermal conversion by means of an optical microscope and the tuning of assembly melting point by selecting an appropriate C_{60} derivative with suitable length or number of alkyl chains. More importantly, considering that SWCNTs are widely used in biology for local heating with operations conducted around body temperature, our results serve as a reminder that NIR irradiation of carbon nanotubes can induce an extreme temperature rise.

1.5   PHOTOCONDUCTIVE SOFT MATERIALS

The covalent functionalization of C_{60} has resulted in the formation of various functional assemblies, including organogels and liquid crystals (LCs). Nakamura *et al.* have reported organogels of alkyl-conjugated C_{60} derivative (**14**, Scheme 1-2) and developed self-assembled nanowires of C_{60} using the Langmuir Blodgett method [49]. The control over solubility of C_{60} obtained by derivatization using an L-glutamide moiety (**15**–**17**, Scheme 1-2) has led to the formation of organogels, especially in mixed organic solvents [50]. In recent years, there has been considerable interest in the design and synthesis of C_{60}-based LC assemblies because of the unique properties resulting from the ordering of different LCs. Deschenaux [51] and Felder-Flesch [52] are the leading contributors in the area of C_{60}-based LCs. The reports from their groups have demonstrated how synthetic design strategies can be utilized to develop plenty of C_{60}-based LCs and to impart anisotropic liquid crystalline character to completely isotropic fullerenes. One of the disadvantages of these systems is that the content of C_{60} part in the liquid crystalline C_{60} derivatives is relatively low, and hence the optoelectronic properties corresponding to C_{60} part will be limited.
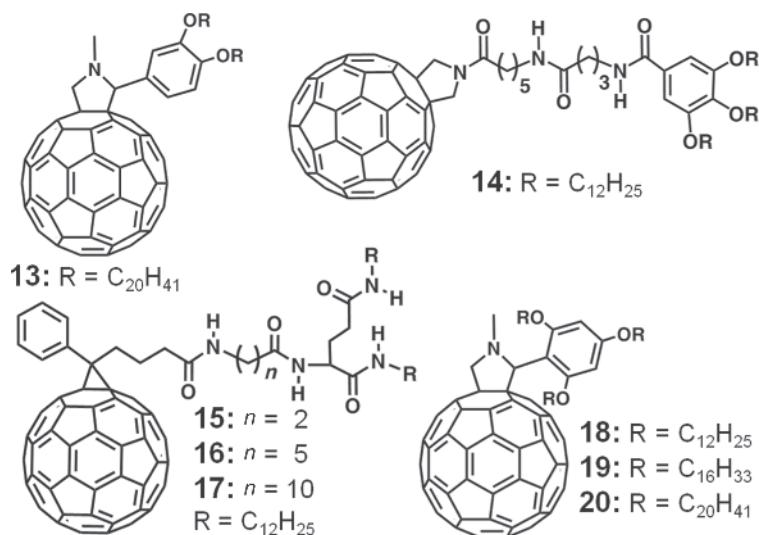
Scheme 1-2 Chemical structures of fulleropyrrolidine functionalized with 3,4-alkyloxyphenyl groups (**13**), 3,4,5-tris(dodecyloxy)benzamide-linked C_{60} organogelator (**14**), C_{60} gelator with L-glutamide moiety (**15–17**), fulleropyrrolidine functionalized with 2,4,6-alkyloxyphenyl groups (**18–20**).

1.5.1 C_{60}-Rich Thermotropic Liquid Crystals

Since C_{60}-based LCs find direct applications in organic photovoltaic devices because of their predetermined, controllable organization at the molecular level, it is extremely important to select the necessary anisotropic building blocks along with C_{60} to attain the preferred ordering. Recently, alkylated C_{60} derivatives, that is, **9, 10, 13** (Schemes 1-1 and 1-2) with a high C_{60} content (up to 50%) and high carrier mobility in the highly ordered mesophase were reported [53]. Polarized optical microscopic (POM) studies of **10** showed a birefringent optical texture (Fig. 1-4a) comparable to smectic phases with a fluid nature in the wide temperature range between 62 and 193°C. An unusual long-range ordered lamellar mesophase in which molecules are assumed to arrange their long axis, on average, perpendicular to the plane of the layers with the C_{60} moieties in a head-to-head configuration was confirmed by the presence of multiple Bragg peaks in the LC state (Fig. 1-4b) [54]. The mesomorphic fullerenes retain reversible electrochemistry as cast films and exhibit electron mobility of $\sim 3 \times 10^{-3}$ cm^2/Vs, which is the largest photoconductivity value for C_{60}-containing LCs. The dense packing of fullerenes carrying the charges is responsible for the high electron mobility observed in the mesophase.

1.5.2 Room Temperature Fullerene Liquids

The advantages of synthetic organic chemistry have been extended to design some room temperature liquid fullerenes. The controlled aggregation of fullerenes at
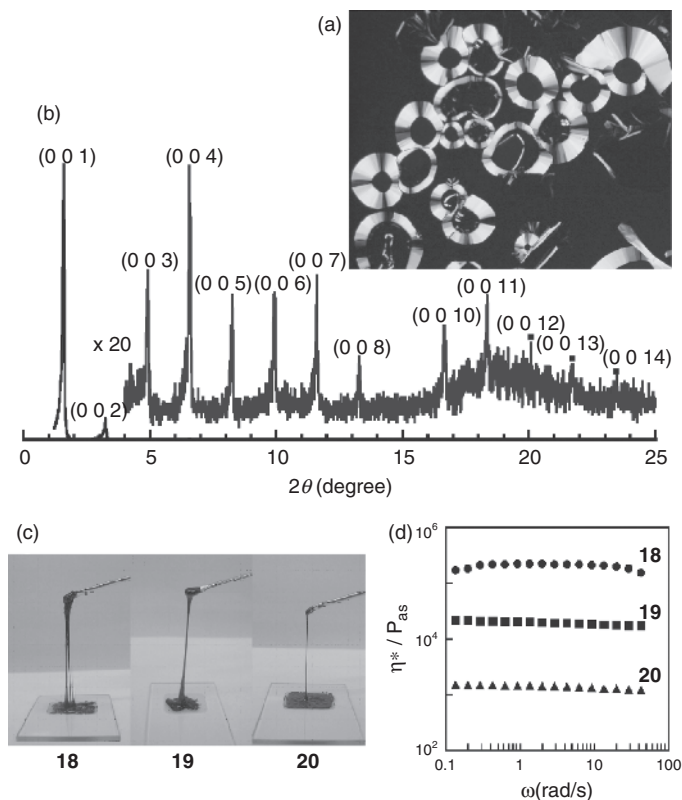
Figure 1-4   (a) Polarized optical micrographic texture of mesophase of **10** at 190°C on cooling from the isotropic phase at a rate of 0.1°C/min and (b) XRD patterns of **10** at 185°C. (c) Photographs of the liquid fullerenes (**18–20**) at room temperature with (d) the corresponding viscosity values. *Source:* Reprinted with permission [53,55].

the molecular level by attaching a 2,4,6-tri(alkyloxy)phenyl group to the fullero-pyrrolidine (**18–20**, Scheme 1-2) resulted in a new kind of nanocarbon fluid matter (Fig. 1-4c) [55]. The substitution pattern and length of alkyl chains were carefully chosen to serve as an effective steric stabilizer, preventing C_{60} aggregation. The lack of perfect molecular ordering in the liquid material is evidenced by very broad peaks in the XRD pattern of the liquid form. The higher loss modulus (G'') value than the storage modulus (G') has confirmed the liquid character of these derivatives at room temperature, and the viscosity of liquid fullerenes can be effectively controlled by changing the alkyl chain length (Fig. 1-4d). An important feature is that liquids with higher alkyl chains show lower viscosity, which is a completely opposite trend to that seen in alkanes. The liquid C_{60} compounds retain the characteristic electrochemical features of C_{60} and carrier mobility of $\sim 3 \times 10^{-2}$ cm^2/Vs (**20** at 20°C). These features make it an extremely attractive novel carbon material for future applications because of the absence of structural defects and quite high C_{60} content.

1.6   CONCLUSIONS

The rational design of covalently functionalized C_{60} derivatives has enlightened the self-assembly of fullerenes. Hence the remarkable achievement in crafting supramorphologies with molecular-level precision using the simple spherical $\pi-\pi$ interaction of fullerenes has gathered much attention. The important criterion in the design of C_{60} derivatives to obtain functional assemblies with a highly ordered C_{60} arrangement and having a high C_{60} content has been realized by alkyl-conjugated fullerenes. In this way, a concept of hydrophobic amphiphilicity through the delicate balance between hydrophobic interactions of the aromatic and aliphatic moieties has been established. The self-organized supramolecular objects exhibited superhydrophobicity, and further robustness of these structures were enhanced through polymerization of the diacetylene unit. Self-assembled microparticles have been used to transfer the nanomorphology to different metal surfaces, enabling the development of metal nanoflakes as highly sensitive SERS surfaces. The incorporation of carbon nanotubes into self-assembly enabled monitoring the temperature rise during photothermal conversion on NIR irradiation. In addition to superhydrophobic characteristics, these molecules revealed the presence of mesophases, with the largest electron mobility reported for C_{60}-containing LCs. The synthetic manipulation of the alkylated fullerenes has ended up with new fluid nanocarbon materials with good photoconductivity. Recent developments in our group have delivered new C_{60} derivatives with better crystallinity and higher C_{60} content. Photoconductive flowerlike supramolecular architectures were developed via self-assembly of a C_{60} derivative (C_{60} content of 84%) bearing a pyridine substituent [56]. Arene–perfluoroarene interaction has been used to develop transparent millimeter-sized flat crystalline C_{60} sheets with anisotropic photoconductivity through 1:1 coassembly of phenyl- and perfluorophenyl-substituted fullerenes [57]. We believe that the control over the morphology of π-conjugated compounds with a high π-core content would be used to diversify their variety of applications in organic electronics.

REFERENCES

1. Lehn, J. M. *Supramolecular Chemistry: Concepts and Perspectives*. VCH, Weinheim, Germany, 1995.

2. Reinhoudt, D. N., Crego-Calama, M. (2002). Synthesis beyond the molecule. *Science*, *295*, 2403–2407.

3. Whitesides, G. M., Grzybowski, B. (2002). Self-assembly at all scales. *Science*, *295*, 2418–2421.

4. Hoeben, F. J. M., Jonkheijm, P., Meijer, E. W., Schenning, A. P. H. J. (2005). About supramolecular assemblies of π-conjugated systems. *Chem. Rev*., *105*, 1491–1546.

5. de Greef, T. F. A., Meijer, E. W. (2008). Supramolecular polymers. *Nature*, *453*, 171–173.

6. Schenning, A. P. H. J., Jonkheijm, P., Hoeben, F. J. M., van Herrikhuyzen, J., Meskers, S. C. J., Meijer, E. W., Herz, L. M., Daniel, C., Silva, C., Phillips, R. T., Friend, R. H., Beljonn, D., Miura, A., Feyter, S. D., Zdanowska, M., Uji-i, H., Schryver, F. C. D., Chen, Z., Würthner, F., Mas-Torrent, M., den Boer, D., Durkut, M., Hadley, P. (2004). Towards supramolecular electronics. *Synth. Met*., *147*, 43–48.

7. Zhang, J., Hoeben, F. J. M., Pouderoijen, M. J., Schenning, A. P. H. J., Meijer, E. W., Schryver, F. C. D., Feyter, S. D. (2006). Hydrogen-bonded oligo(*p*-phenylenevinylene) functionalized with perylene bisimide: self-assembly and energy transfer. *Chem.—Eur. J.*, *12*, 9046–9055.

8. Katsonis, N., Xu, H., Haak, R. M., Kudernac, T., Tomović, Ž., George, S., Van der Auweraer, M., Schenning, A. P. H. J., Meijer, E. W., Feringa, B. L., Feyter, S. D. (2008). Emerging solvent-induced homochirality by the confinement of achiral molecules against a solid surface. *Angew. Chem. Int. Ed.*, *47*, 4997–5001.

9. Ajayaghosh, A., Praveen, V. K. (2007). π-Organogels of self-assembled *p*-phenylenevinylenes: soft materials with distinct size, shape, and functions. *Acc. Chem. Res.*, *40*, 644–656.

10. Ajayaghosh, A., Praveen, V. K., Vijayakumar, C. (2008) Organogels as scaffolds for excitation energy transfer and light harvesting. *Chem. Soc. Rev.*, *37*, 109–122.

11. Würthner, F. (2004). Perylene bisimide dyes as versatile building blocks for functional supramolecular architectures. *Chem. Commun.*, *14*, 1564–1579.

12. Kronenberg, N. M., Deppisch, M., Würthner, F., Lademann, H. W. A., Deinga, K., Meerholz, K. (2008). Bulk heterojunction organic solar cells based on merocyanine colorants. *Chem. Commun.*, 6489–6491.

13. Hill, J. P., Jin, W., Kosaka, A., Fukushima, T., Ichihara, H., Shimomura, T., Ito, K., Hashizume, T., Ishii, N., Aida, T. (2004). Self-assembled hexa-*peri*-hexabenzocoronene graphitic nanotube. *Science*, *304*, 1481–1483.

14. Tashiro, K., Aida, T. (2007). Metalloporphyrin hosts for supramolecular chemistry of fullerenes. *Chem. Soc. Rev.*, *36*, 189–197.

15. Kato, T., Mizoshita, N., Kishimoto, K. (2006). Functional liquid-crystalline assemblies: self-organized soft materials. *Angew. Chem. Int. Ed.*, *45*, 38–68.

16. Babu, S. S., Möhwald, H., Nakanishi, T. (2010). Recent progress in morphology control of supramolecular fullerene assemblies and its applications. *Chem. Soc. Rev.*, *39*, 4021–4035.

17. Segura, J. L., Martín, N., Guldi, D. M. (2005). Materials for organic solar cells: the C_{60}/π-conjugated oligomer approach. *Chem. Soc. Rev.*, *34*, 31–47.

18. López, A. M., Mateo-Alonsobc, A., Prato, M. (2011). Materials chemistry of fullerene C_{60} derivatives. *J. Mater. Chem.*, *21*, 1305–1318.

19. Asanuma, H., Li, H., Nakanishi, T., Möhwald, H. (2010). Fullerene derivatives that bear aliphatic chains as unusual surfactants: hierarchical self-organization, diverse morphologies, and functions. *Chem.—Eur. J.*, *16*, 9330–9338.

20. Israelachvili, J., *Intermolecular and Surface Forces*. Academic Press, London, 1991.

21. Fuhrhop, J.-H., Helfrich, W. (1993). Fluid and solid fibers made of lipid molecular bilayers. *Chem. Rev.*, *93*, 1565–1582.

22. Hafkamp, R. J. H., Feiters, M. C., Nolte, R. J. M. (1994). Tunable supramolecular structures from a gluconamide containing imidazole. *Angew. Chem. Int. Ed. Engl.*, *33*, 986–987.

23. Löwik, D. W. P. M., van Hest, J. C. M. (2004). Peptide based amphiphiles. *Chem. Soc. Rev.*, *33*, 234–245.

24. Elemans, J. A. A. W., Rowan, A. E., Nolte, R. J. M. (2003). Mastering molecular matter. Supramolecular architectures by hierarchical self-assembly. *J. Mater. Chem.*, *13*, 2661–2670.

25. Zhou, S., Burger, C., Chu, B., Sawamura, M., Nagahama, N., Toganoh, M., Hackler, U. E., Isobe, H., Nakamura, E. (2001). Spherical bilayer vesicles of fullerene-based surfactants in water: a laser light scattering study. *Science*, *291*, 1944–1947.

26. Zhang, G., Liu, Y., Liang, D., Gan, L., Li, Y. (2010). Facile synthesis of isomerically pure fullerenols and formation of spherical aggregates from $C_{60}(OH)_8$. *Angew. Chem. Int. Ed.*, *49*, 5293–5295.

27. Cassell, A. M., Asplund, C. L., Tour, J. M. (1999). Self-assembling supramolecular nanostructures from a C60 derivative: nanorods and vesicles. *Angew. Chem. Int. Ed.*, *38*, 2403–2405.

28. Shiga, T., Motohiro, T. (2007). Supramolecular structures formed by the self assembly of ionic fullerenes in binary liquid mixtures. *J. Mater. Res.*, *22*, 3029–3035.

29. Brough, P., Bonifazi, D., Prato, M. (2006). Self-organization of amphiphilic [60]fullerene derivatives in nanorod-like morphologies. *Tetrahedron*, *62*, 2110–2114.

30. Nakanishi, T., Schmitt, W., Michinobu, T., Kurth, D. G., Ariga, K. (2005). Hierarchical supramolecular fullerene architectures with controlled dimensionality. *Chem. Commun.*, 5982–5984.

31. Murakami, H., Watanabe, Y., Nakashima, N. (1996). Fullerene lipid chemistry: self-organised multilayer films of a C60-bearing lipid with main and subphase transitions. *J. Am. Chem. Soc*., *118*, 4484–4485.

32. Nakanishi, T., Morita, M., Murakami, H., Sagara, T., Nakashima, N. (2002). Structure and electrochemistry of self-organized fullerene-lipid bilayer films. *Chem.—Eur. J*., *8*, 1641–1648.

33. Mouri, E., Nakanishi, T., Nakashima, N., Matsuoka, H. (2002). Nanostructure of fullerene-bearing artificial lipid monolayer on water surface by *in situ* X-ray reflectometry. *Langmuir*, *18*, 10042–10045.

34. Gayathri, S. S., Agarwal, A. K., Suresh, K. A., Patnaik, A. (2005). Structure and synamics in solvent-polarity-induced aggregates from a C$_{60}$ fullerene-based dyad. *Langmuir*, *21*, 12139–12145.

35. Gayathri, S. S., Patnaik, A. (2007). Aggregation of a C$_{60}$-didodecyloxybenzene dyad: structure, dynamics, and mechanism of vesicle growth. *Langmuir*, *23*, 4800–4808.

36. Nakanishi, T. (2010). Supramolecular soft and hard materials based on self-assembly algorithms of alkyl-conjugated fullerenes. *Chem. Commun*., *46*, 3425–3436.

37. Nakanishi, T., Ariga, K., Michinobu, T., Yoshida, K., Takahashi, H., Teranishi, T., Möhwald, H., Kurth, D. G. (2007). Flower-shaped supramolecular assemblies: hierarchical organization of a fullerene bearing long aliphatic chains. *Small*, *3*, 2019–2023.

38. Nakanishi, T., Wang, J., Möhwald, H., Kurth, D. G., Michinobu, T., Takeuchi, M., Ariga, K. (2009). Supramolecular shape shifter: polymorphs of self-organised fullerene assemblies. *J. Nanosci. Nanotechnol*., *9*, 550–556.

39. Nakanishi, T., Miyashita, N., Michinobu, T., Wakayama, Y., Tsuruoka, T., Ariga, K., Kurth, D. G. (2006). Perfectly straight nanowires of fullerenes bearing long alkyl chains on graphite. *J. Am. Chem. Soc*., *128*, 6328–6329.

40. Nakanishi, T., Takahashi, H., Michinobu, T., Takeuchi, M., Teranishi, T., Ariga, K. (2008). Fullerene nanowires on graphite: epitaxial self-organisations of a fullerene bearing double long-aliphatic chains. *Colloids Surf., A: Physicochem. Eng. Aspects*, *321*, 99–105.

41. Li, X.-M., Reinhoudt, D., Crego-Calama, M. (2007). What do we need for a superhydrophobic surface? A review on the recent progress in the preparation of superhydrophobic surfaces. *Chem. Soc. Rev*., *36*, 1350–1368.

42. Nakanishi, T., Michinobu, T., Yoshida, K., Shirahata, N., Ariga, K., Möhwald, H., Kurth, D. G. (2008). Nanocarbon superhydrophobic surfaces created from fullerene-based hierarchical supramolecular assemblies. *Adv. Mater.*, *20*, 443–446.

43. Nakanishi, T., Shen, Y., Wang, J., Li, H., Fernandes, P., Yoshida, K., Yagai, S., Takeuchi, M., Ariga, K., Kurth, D. G., Möhwald, H. (2010). Superstructures and superhydrophobic property in hierarchical organized architectures of fullerenes bearing long alkyl tails. *J. Mater. Chem*., *10*, 1253–1260.

44. Wang, J., Shen, Y., Kessel, S., Fernandes, P., Yoshida, K., Yagai, S., Kurth, D. G., Möhwald, H., Nakanishi, T. (2009). Self-assembly made durable: water-repellent materials formed by cross-linking fullerene derivatives. *Angew. Chem. Int. Ed*., *48*, 2166–2170.

45. Shen, Y., Wang, J., Kuhlmann, U., Hildebrandt, P., Ariga, K., Möhwald, H., Kurth, D. G., Nakanishi, T. (2009). Supramolecular templates for nanoflake-metal surfaces. *Chem.—Eur. J*., *15*, 2763–2767.

46. Sezer, M., Feng, J.-J., Ly, H. K., Shen, Y., Nakanishi, T., Kuhlmann, U., Hildebrandt, P., Möhwald, H., Weidinger, I. M. (2010). Multi-layer electron transfer across nanostructured Ag-SAM-Au-SAM junctions probed by surface enhanced Raman spectroscopy. *Phys. Chem. Chem. Phys*., *12*, 9822–9829.

47. Singh, P., Campidelli, S., Giordani, S., Bonifazi, D., Biancoa, A., Prato, M. (2009). Organic functionalisation and characterisation of single-walled carbon nanotubes. *Chem. Soc. Rev*., *38*, 2214–2230.

48. Shen, Y., Skirtach, A. G., Seki, T., Yagai, S., Li, H., Möhwald, H., Nakanishi, T. (2010). Assembly of fullerene-carbon nanotubes: temperature indicator for photothermal conversion. *J. Am. Chem. Soc*., *132*, 8566–8568.

49. Tsunashima, R., Noro, S.-I., Akutagawa, T., Nakamura, T., Kawakami, H., Toma, K. (2008). Fullerene nanowires: self-assembled structures of a low-molecular-weight organogelator fabricated by the Langmuir-Blodgett method. *Chem.—Eur. J*., *14*, 8169–8176.

50. Watanabe, N., Jintoku, H., Sagawa, T., Takafuji, M., Sawada, T., Ihara, H. (2009). Self-assembling fullerene derivatives for energy transfer in molecular gel system. *J. Phys.: Conf. Ser*., *159*, 012016.

51. Campidelli, S., Bourgun, P., Guintchin, B., Furrer, J., Stoeckli-Evans, H., Saez, I. M., Goodby, J. W., Deschenaux, R. (2010). Diastereoisomerically pure fulleropyrrolidines as chiral platforms for the design of optically active liquid crystals. *J. Am. Chem. Soc*., *132*, 3574–3581.

52. Mamlouk, H., Heinrich, B., Bourgogne, C., Donnio, B., Guillon, D., Felder-Flesch, D. (2007). A nematic [60]fullerene supermolecule: when polyaddition leads to supramolecular self-organization at room temperature. *J. Mater. Chem*., *17*, 2199–2205.

53. Nakanishi, T., Shen, Y., Wang, J., Yagai, S., Funahashi, M., Kato, T., Fernandes, P., Möhwald, H., Kurth, D. G. (2008). Electron transport and electrochemistry of mesomorphic fullerenes with long-range ordered lamellae. *J. Am. Chem. Soc*., *130*, 9236–9237.

54. Fernandes, P. A. L., Yagai, S., Möhwald, H., Nakanishi, T. (2010). Molecular arrangement of alkylated fullerenes in the liquid crystalline phase studied with X-ray diffraction. *Langmuir*, *26*, 4339–4345.

55. Michinobu, T., Nakanishi, T., Hill, J. P., Funahashi, M., Ariga, K. (2006). Room temperature liquid fullerenes: an uncommon morphology of C_{60} derivatives. *J. Am. Chem. Soc*., *128*, 10384–10385.

56. Zhang, X., Nakanishi, T., Ogawa, T., Saeki, A., Seki, S., Shen, Y., Yamauchi, Y., Takeuchi, M. (2010). Flowerlike supramolecular architectures assembled from C_{60} equipped with a pyridine substituent. *Chem. Commun*., *46*, 8752–8754.

57. Babu, S. S., Saeki, A., Seki, S., Möhwald, H., Nakanishi, T. (2011). Millimeter-sized flat crystalline sheet architectures of fullerene assemblies with anisotropic photoconductivity. *Phys. Chem. Chem. Phys*., *13*, 4830–4834.